ELSEVIER

Engineering Analysis with Boundary Elements 29 (2005) 59–75

ENGINEERING ANALYSIS *with* BOUNDARY ELEMENTS

www.elsevier.com/locate/enganabound

Particular solutions of Laplace's equations on polygons and new models involving mild singularities

Zi-Cai Li[a,b], Tzon-Tzer Lu[a], Hsin-Yun Hu[c], Alexander H.D. Cheng[d,*]

[a]*Department of Applied Mathematics, National Sun Yat-sen University, Kaohsiung 80424, Taiwan, ROC*
[b]*Department of Computer Science and Engineering, National Sun Yat-sen University, Kaohsiung 80424, Taiwan, ROC*
[c]*National Center for Theoretical Sciences Mathematics Division, National Tsing Hua University, Hsinchu 30043, Taiwan, ROC*
[d]*Department of Civil Engineering, University of Mississippi, 203 Carrier Hall, University, MS 38677, USA*

Available online 24 November 2004

Abstract

In this paper, the harmonic functions of Laplace's equations are derived explicitly for the Dirichlet and the Neumann boundary conditions on the boundary of a sector. Those harmonic functions are more explicit than those of Volkov [Volkov EA, Block method for solving the Laplace equation and for constructing conformal mappings. Boca Raton: CRC Press; 1994], and easier to expose the mild singularity at the domain corners of the Laplace solutions. Moreover, the particular solutions of Poisson's equation on the polygon is also provided. We also explore in detail the singularities of the polygons with the boundary angles $\Theta=\pi/2$, $3\pi/2$, π and 2π, which often occur in many testing models.

Besides, the popular singularity models, Motz's and the cracked beam problems in Lu et al. [Lu TT, Hu HY, Li ZC. Highly accurate solutions of Motz's and the cracked beam problems. Eng Anal Bound Elem; 2004, in press], we design two new singularity models, one with discontinuous singularity, and the other with crack plus mild singularities. The collocation Trefftz method, the Schwarz alternating method, and their combinations may be chosen to seek the solution with high accuracy, which may be used to test other numerical methods. The particular solutions of the Laplace equations and their singularities are fundamental to numerical partial differential equations in both algorithms and error analysis.

Keywords: Laplace's equation; Singularity; Particular solutions; Collocation method; Trefftz method; Schwarz alternating method; Combined method

AMS(MOS) Subject classification: 65N10; 65N30

1. Introduction

In this paper, we derive explicitly the particular solutions of Laplace's equation in sectors with the Dirichlet, Neumann, and their mixed boundary conditions. We explore those in particular with the boundary angles of $\Theta=\pi/2$, $3\pi/2$, π and 2π, which often occur in Motz's problem, the L-shaped and the cracked beam problems. Although the particular solutions in this paper may be found in Volkov [11,12], the formulas of the particular solutions given in this paper are more explicit than those of Volkov [12], and easier to expose the mild singularity at the domain corners of the Laplace solutions. Moreover, new models are designed for Laplace's equations including discontinuity, and the cracked plus mild singularities, $r^k \ln r$, and the Trefftz method using the piecewise particular solutions can provide highly accurate solutions, which may be used to test other numerical methods.

When a solution domain can be split into several subdomains, the local particular solutions in each subdomain can be found in this paper. Several methods for Laplace's equations with highly accurate solutions may be chosen: (1) the collocation Trefftz methods (i.e. the boundary approximation method in [5]), (2) the combinations of the collocation Trefftz and the Schwarz alternating methods, and (3) other methods such as the block method in [11,12].

This paper is organized as follows. In Section 2, the particular solutions are derived for Laplace's equations in

* Corresponding author. Tel.: +1 662 9155362; fax: +1 662 9155523.
E-mail address: acheng@olemiss.edu (A.H.D. Cheng).

0955-7997/$ - see front matter © 2004 Elsevier Ltd. All rights reserved.
doi:10.1016/j.enganabound.2004.09.005

sectors with the Dirichlet boundary conditions, and their explicit formulas are provided for special angles Θ. In Section 3, the particular solutions of those involving the Neumann boundary conditions are discussed. In Section 4, the particular solutions of Poisson's equation are provided, and those are developed for the cases that the boundary functions of the Dirichlet and the Neumann boundary conditions are not smooth. Besides, the singularities of the solutions at the boundary angles $\Theta=\pi/2$, $3\pi/2$, π and 2π are especially analyzed. In Section 5, two new models, one with discontinuity, and other with crack plus mild singularities, are designed, and the collocation Trefftz method are used to provide their very accurate solutions.

2. The harmonic functions

Consider the Laplace equation with the Dirichlet boundary conditions (see Fig. 1)

$$\Delta u = \left(\frac{\partial^2 u}{\partial x^2} + \frac{\partial^2 u}{\partial y^2}\right) = 0, \quad \text{in } S^*, \tag{2.1}$$

$$u = g, \quad \text{on } \partial S^*, \tag{2.2}$$

where S^* is a polygon. For each angle, we seek the harmonic solutions in the corresponding sectorial domain (see Fig. 2) $S=\{(r,\theta), 0<r<R, 0<\theta<\Theta\}$:

$$\Delta u = 0, \quad \text{in } S.$$

We suppose that the function g is highly smooth that it can be expressed by the power series

$$u|_{\bar{OA}} = g|_{\bar{OA}} = \sum_{i=0}^{\infty} \alpha_i r^i, \quad 0 \le r \le R, \ \theta = 0, \tag{2.3}$$

$$u|_{\bar{OB}} = g|_{\bar{OB}} = \sum_{i=0}^{\infty} \beta_i r^i, \quad 0 \le r \le R, \ \theta = \Theta, \tag{2.4}$$

where β_i and α_i are known coefficients. In fact, when the function $g|_{\bar{OB}} = g_1(r)$ is highly smooth, it can be expanded by Taylor's series:

$$g_1(r) = \sum_{i=0}^{\infty} \frac{g_1^{(i)}(0) r^i}{i!}.$$

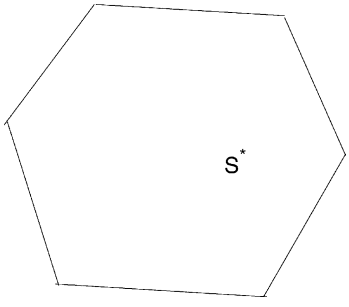

Fig. 1. A polygonal domain.

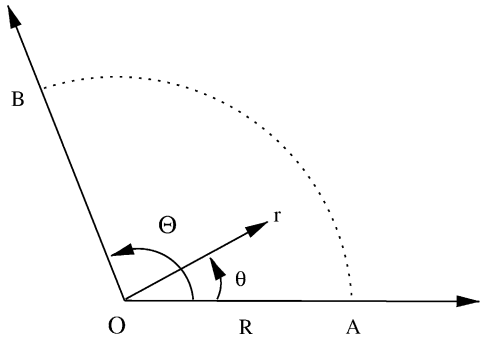

Fig. 2. A sectorial domain.

Then $\beta_i = g_1^{(i)}(0)/i!$. Similarly, for $g|_{\bar{OA}} = g_0(r)$, we also have:

$$g_0(r) = \sum_{i=0}^{\infty} \frac{g_0^{(i)}(0) r^i}{i!}.$$

Hence, for any smooth Dirichlet boundary condition $u=g$ on ∂S, we may simply consider the following case in S (see Fig. 3). In this paper, we also assume that the corresponding series occurring are also convergent in the desired domain. Otherwise, we may consider only the polynomial boundary conditions

$$u|_{\bar{OA}} = g|_{\bar{OA}} = \sum_{i=0}^{M} \alpha_i r^i, \quad 0 \le r \le R, \ \theta = 0, \tag{2.5}$$

$$u|_{\bar{OB}} = g|_{\bar{OB}} = \sum_{i=0}^{N} \beta_i r^i, \quad 0 \le r \le R, \ \theta = \Theta, \tag{2.6}$$

where β_i and α_i are known coefficients. This is the special case of (2.3) and (2.4), because we may let $\beta_i=0$ as $i>N$ and $\alpha_i=0$ as $i>M$.

Let us consider the mixed type of the Dirichlet–Neumann boundary conditions in Fig. 4

$$\Delta u = 0, \ \text{in } S, \quad u = g_D, \ \text{on } \Gamma_D, \quad \frac{\partial u}{\partial n} = g_N, \ \text{on } \Gamma_N, \tag{2.7}$$

where $\partial S = \Gamma_D \cup \Gamma_N$ and n is the outnormal of ∂S. There are four types of mixed boundary conditions on two adjacent

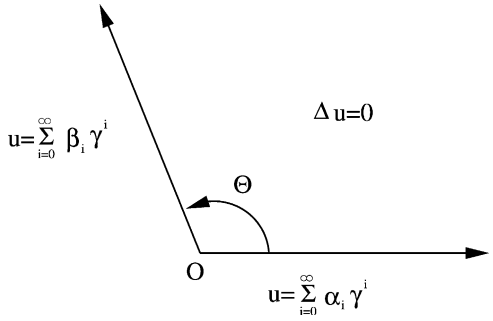

Fig. 3. The Dirichlet boundary conditions.

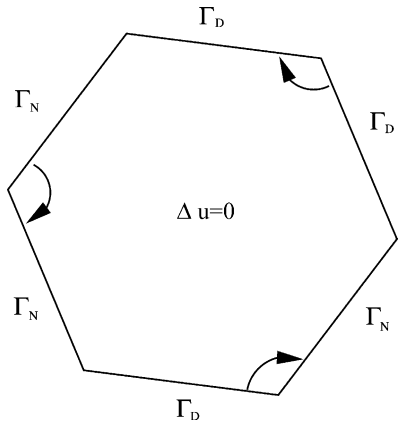

Fig. 4. A polygon.

edges of a corner: (1) the D–D type, (2) the N–D type, (3) the D–N type, and (4) the N–N type.

The harmonic solutions of the D–D type will be derived in this section, and those of the N–D, D–N and N–N types in the next section.

2.1. General cases

The general solutions of Laplace's equation in S satisfying (2.3) and (2.4) can be split into $\bar{u}$ and u_g

$$u = \bar{u} + u_g, \tag{2.8}$$

where the general solutions u_g satisfy

$$\Delta u_g = 0, \ \text{in } S, \quad u_g = 0, \ \theta = 0 \ \text{and} \ \theta = \Theta, \tag{2.9}$$

where $0<\Theta\leq 2\pi$, and the particular solution $\bar{u}$ satisfies:

$$\Delta \bar{u} = 0, \ \text{in } S, \tag{2.10}$$

$$\bar{u}|_{\theta=0} = \sum_{i=0}^{\infty} \alpha_i r^i, \quad \bar{u}|_{\theta=\Theta} = \sum_{i=0}^{\infty} \beta_i r^i. \tag{2.11}$$

Note that in (2.9) and (2 10), the boundary condition on $\ell_R=\{(r,\theta)|r=R, 0\leq\theta\leq\Theta\}$ has not been given yet. Hence, the general solutions u_g and u are not unique.

First for (2.9), the general solutions are $\phi_i=r^{\sigma i}\sin\sigma_i\theta$, $\phi_i|_{\theta=0}=0$ holds automatically, and $\phi_i|_{\theta=\Theta}=0$ leads to $\sin\sigma_i\Theta=0$. Hence, $\sigma_i\Theta=i\pi$, i.e. $\sigma_i=i\pi/\Theta$. We obtain the general solutions

$$u_g = \sum_{i=0}^{\infty} c_i r^{i\pi/\Theta} \sin\left(\frac{i\pi}{\Theta}\theta\right), \tag{2.12}$$

where c_i are the coefficients to be found.

First, we seek the particular solutions involving mild singularity $r^k \ln r$, $k=1, 2,\ldots$ The *mild* singularity is investigated in this paper, to compare with the rather strong singularity $O(r^\gamma)$, $0<\gamma<1$. Consider a complex variable z, and let $z=x+\mathrm{i}y=r\,\mathrm{e}^{\mathrm{i}\theta}$. The real and imaginary parts of the complex functions, $z^p \ln z$, $p\in\mathbf{R}$ are harmonic. We then have

$$\begin{aligned} z^p \ln z &= (r^p\cos p\theta + \mathrm{i}r^p\sin p\theta)\times(\ln r + \mathrm{i}\theta) \\ &= r^p\{\ln r\cos p\theta - \theta\sin p\theta\} \\ &\quad + \mathrm{i}r^p\{\ln r\sin p\theta + \theta\cos p\theta\}, \end{aligned}$$

where p is a real number. Hence the following functions are also harmonic:

$$\varphi_p = \varphi_p(r,\theta) = r^p\{\ln r\sin p\theta + \theta\cos p\theta\}, \tag{2.13}$$

$$\psi_p = \psi_p(r,\theta) = r^p\{\ln r\cos p\theta - \theta\sin p\theta\}. \tag{2.14}$$

When p is a positive integer k, $k=1,2,\ldots$, we denote:

$$\varphi_k = \varphi_k(r,\theta) = r^k\{\ln r\sin k\theta + \theta\cos k\theta\}, \tag{2.15}$$

$$\psi_k = \psi_k(r,\theta) = r^k\{\ln r\cos k\theta - \theta\sin k\theta\}. \tag{2.16}$$

Define the functions

$$\Phi_i = \Phi_i(r,\theta) = \begin{cases} \dfrac{r^i\sin i\theta}{\sin i\Theta}, & \text{if } i\Theta \neq k\pi, \ k=1,2,\ldots \\ \dfrac{(-1)^k}{\Theta}\varphi_i(r,\theta), & \text{if } i\Theta = k\pi \text{ for some } k, \end{cases} \tag{2.17}$$

where $i\geq 1$ and $\phi_i(r,\theta)$ is given in (2.15). Hence, we have:

$$\Phi_i|_{\theta=0} = 0, \quad \Phi_i|_{\theta=\Theta} = r^i, \ \forall\, r>0, \ i=1,2,\ldots \tag{2.18}$$

Choose the particular solutions for (2.10) and (2.11) as the following form

$$\bar{u} = \sum_{i=0}^{\infty} A_i r^i\cos i\theta + B_0\theta + \sum_{i=1}^{\infty} B_i\Phi_i(r,\theta), \tag{2.19}$$

where the coefficients A_i and B_i are to be determined below. When $\theta=0$ we have $A_i=\alpha_i$ from the boundary condition in (2.11), and when $\theta=\Theta$:

$$A_0 + B_0\Theta = \beta_0, \quad A_i\cos i\Theta + B_i = \beta_i, \ i=1,2,\ldots \tag{2.20}$$

Hence we obtain the coefficients:

$$B_0 = \frac{\beta_0-\alpha_0}{\Theta}, \quad B_i = \beta_i - \alpha_i\cos i\Theta, \ i=1,2,\ldots \tag{2.21}$$

Substituting (2.21) into (2.19) gives the particular solutions:

$$\bar{u} = \frac{\beta_0-\alpha_0}{\Theta}\theta + \sum_{i=0}^{\infty}\alpha_i r^i\cos i\theta + \sum_{i=1}^{\infty}(\beta_i - \alpha_i\cos i\Theta)\Phi_i(r,\theta). \tag{2.22}$$

In Volkov [12], the following form of particular solutions for (2.10) and (2.11) are given by

$$\bar{u} = \alpha_0 + \frac{\beta_0 - \alpha_0}{\Theta}\theta + \sum_{i=1}^{\infty} \alpha_i \bar{\Phi}_i(r,\theta) \sum_{i=1}^{\infty} \beta_i \Phi_i(r,\theta), \tag{2.23}$$

where

$$\bar{\Phi}_i = \bar{\Phi}_i(r,\theta) = \Phi_i(r,\Theta - \theta), \tag{2.24}$$

to satisfy:

$$\bar{\Phi}_i|_{\theta=\Theta} = 0, \quad \bar{\Phi}_i|_{\theta=0} = r^i, \ \forall\, r > 0,\ i = 1,2,\ldots$$

First, let us show the equivalence between (2.22) and (2.23). When $\Theta \neq k\pi/i$, $i \geq 1$, we have from (2.23):

$$\bar{u} = \alpha_0 + \frac{\beta_0 - \alpha_0}{\Theta}\theta + \sum_{i=1}^{\infty} \alpha_i r^i \frac{\sin i(\Theta - \theta)}{\sin i\Theta} + \sum_{i=1}^{\infty} \beta_i \frac{r^i \sin i\theta}{\sin i\Theta}. \tag{2.25}$$

Since $\sin i(\Theta - \theta) = \sin i\Theta \cos i\theta - \sin i\theta \cos i\Theta$, we obtain from the above equation:

$$\bar{u} = \frac{\beta_0 - \alpha_0}{\Theta}\theta + \sum_{i=0}^{\infty} \alpha_i r^i \cos i\theta + \sum_{i=1}^{\infty} (\beta_i - \alpha_i \cos i\Theta) r^i \frac{\sin i\theta}{\sin i\Theta}. \tag{2.26}$$

This is the very (2.22) for $\Theta \neq k\pi/i$.

When $i\Theta = k\pi$ for some k, to confirm the equivalence between (2.22) and (2.23), it suffices to show:

$$\bar{\Phi} = r^i \cos i\theta - \cos i\Theta \Phi_i. \tag{2.27}$$

In fact, we have from (2.24) and (2.17)

$$\bar{\Phi}(r,\theta) = \Phi(r,\Theta - \theta)$$

$$= r^i \frac{(-1)^k}{\Theta} (\ln r \sin i(\Theta - \theta) + (\Theta - \theta)\cos i(\Theta - \theta)). \tag{2.28}$$

When $i\Theta = k\pi$, there exist the equalities:

$$\sin i(\Theta - \theta) = \sin i\Theta \cos i\theta - \cos i\Theta \sin i\theta = (-1)^{k+1} \sin i\theta, \tag{2.29}$$

$$\cos i(\Theta - \theta) = \cos i\Theta \cos i\theta + \sin i\Theta \sin i\theta = (-1)^k \cos i\theta. \tag{2.30}$$

Substituting (2.29) and (2.30) into (2.28) gives the desired result (2.27).

Second, Volkov in [12] also considers the case of $i\Theta \neq k\pi$ but $i\Theta \approx k\pi$ so that the ratio $\sin i\theta / \sin i\Theta$ becomes very large. Other basic functions are also introduced in [12] for the case of $0 < |\sin i\Theta| < 1/2$. This is interesting for theory but not for application. In practical engineering problems, usually we may assume $\Theta = (K/L)\pi$, $0 < K \leq 2L$, and L and K are two integers of relatively prime and in moderate size. Then we have

$$\min_i |\sin i\Theta| = \min_i |\sin \frac{iK}{L}\pi| = |\sin \frac{\pi}{L}| \approx \frac{\pi}{L},$$

over all positive integers i such that $i\Theta/\pi$ is not an integer. Hence, the ratio

$$\max_i \left| \frac{\sin i\theta}{\sin i\Theta} \right| \leq \frac{L}{\pi},$$

will not be very large. Consequently, we omit the case of $i\Theta \approx k\pi$ in this paper.

Third, let us compare the formulas of the functions (2.22), and (2.23) of Volkov. Eq. (2.23) is clearly symmetric with respect to $\theta = \Theta/2$. In contrast, we may rewrite (2.22) as

$$\bar{u} = \alpha_0 + \frac{\beta_0 - \alpha_0}{\Theta}\theta + \sum_{i=1}^{\infty} \alpha_i (r^i \cos i\theta - \cos i\Theta \Phi_i(r,\theta)) + \sum_{i=1}^{\infty} \beta_i \Phi_i(r,\theta), \tag{2.31}$$

which is not symmetric, indeed. From the viewpoint of computation, both (2.22) and (2.23) are effective. However, Eqs. (2.22) and (2.31) are more explicit. In particular, Eq. (2.22) displays straightforward the mild singularity. For instance, when $i\Theta = k\pi$ and $\beta_i \neq \alpha_i \cos i\Theta$, there does exist a mild singularity of $O(r^i \ln r)$. More exploration on the mild singularity is provided in Section 4.3.

Remark 2.1. It is assumed that the series in (2.31) is convergent. Otherwise, we may consider only the finite terms in (2.11):

$$\bar{u}|_{\theta=0} = \sum_{i=0}^{M} \alpha_i r^i, \quad \bar{u}|_{\theta=\Theta} = \sum_{i=0}^{N} \beta_i r^i. \tag{2.32}$$

Hence, the solutions become

$$\bar{u} = \alpha_0 + \frac{\beta_0 - \alpha_0}{\Theta}\theta + \sum_{i=1}^{M} \alpha_i (r^i \cos i\theta - \cos i\Theta \Phi_i(r,\theta)) + \sum_{i=1}^{N} \beta_i \Phi_i(r,\theta), \tag{2.33}$$

to replace (2.31). Similarly for all infinite series given below, it is always assumed that they are convergent. Otherwise, a suitable modification should be made correspondingly.

2.2. Formulas for special Θ

Based on (2.22) and (2.17), we list the particular solutions which are often used in application.

(1) When $\Theta = \pi$:

$$\bar{u} = \frac{\beta_0 - \alpha_0}{\pi}\theta + \sum_{i=0}^{\infty} \alpha_i r^i \cos i\theta + \sum_{i=1}^{\infty} \frac{(-1)^i \beta_i - \alpha_i}{\pi} \varphi_i(r,\theta). \tag{2.34}$$

(2) When $\Theta=2\pi$:

$$\bar{u}=\frac{\beta_0-\alpha_0}{2\pi}\theta+\sum_{i=0}^{\infty}\alpha_i r^i\cos i\theta+\sum_{i=1}^{\infty}\frac{\beta_i-\alpha_i}{2\pi}\varphi_i(r,\theta). \tag{2.35}$$

(3) When $\Theta=\pi/2$:

$$\begin{aligned}\bar{u}=&\frac{2(\beta_0-\alpha_0)}{\pi}\theta+\sum_{i=0}^{\infty}\alpha_i r^i\cos i\theta\\&+\sum_{j=0}^{\infty}(-1)^j\beta_{2j+1}r^{2j+1}\sin(2j+1)\theta\\&+\sum_{j=1}^{\infty}\frac{2}{\pi}((-1)^j\beta_{2j}-\alpha_{2j})\varphi_{2j}(r,\theta).\end{aligned} \tag{2.36}$$

(4) When $\Theta=3\pi/2$:

$$\begin{aligned}\bar{u}=&\frac{2(\beta_0-\alpha_0)}{3\pi}\theta+\sum_{i=0}^{\infty}\alpha_i r^i\cos i\theta\\&+\sum_{j=0}^{\infty}(-1)^{j+1}\beta_{2j+1}r^{2j+1}\sin(2j+1)\theta\\&+\sum_{j=1}^{\infty}\frac{2}{3\pi}((-1)^j\beta_{2j}-\alpha_{2j})\varphi_{2j}(r,\theta).\end{aligned} \tag{2.37}$$

Note that the formulas of the particular solutions for $\Theta=\pi$ and $\Theta=2\pi$ are very close, and so are those for $\Theta=\pi/2$ and $\Theta=3\pi/2$. Except the different angles Θ, the only difference is that the sign $(-1)^i$ may change in the series of β_i.

(5) When $\Theta=\pi/3, 2\pi/3, 4\pi/3, 5\pi/3$:

$$\begin{aligned}\bar{u}=&\frac{\beta_0-\alpha_0}{\Theta}\theta+\sum_{i=0}^{\infty}\alpha_i r^i\cos i\theta\\&+\sum_{j=0}^{\infty}\frac{\beta_{3j+1}-\alpha_{3j+1}\cos(3j+1)\Theta}{\sin(3j+1)\Theta}r^{3j+1}\sin(3j+1)\theta\\&+\sum_{j=0}^{\infty}\frac{\beta_{3j+2}-\alpha_{3j+2}\cos(3j+2)\Theta}{\sin(3j+2)\Theta}r^{3j+2}\sin(3j+2)\theta\\&+\sum_{j=1}^{\infty}\frac{1}{\Theta}(\beta_{3j}\cos 3j\Theta-\alpha_{3j})\varphi_{3j}(r,\theta).\end{aligned}$$

(6) When $\Theta=\pi/4, 3\pi/4, 5\pi/4, 7\pi/4$:

$$\begin{aligned}\bar{u}=&\frac{\beta_0-\alpha_0}{\Theta}\theta+\sum_{i=0}^{\infty}\alpha_i r^i\cos i\theta\\&+\sum_{j=0}^{\infty}\sum_{k=1}^{3}\frac{\beta_{4j+k}-\alpha_{4j+k}\cos(4j+k)\Theta}{\sin(4j+k)\Theta}r^{4j+k}\sin(4j+k)\theta\\&+\sum_{j=1}^{\infty}\frac{1}{\Theta}(\beta_{4j}\cos 4j\Theta-\alpha_{4j})\varphi_{4j}(r,\theta).\end{aligned}$$

(7) When $\Theta=(K/L)\pi$, $0<K<2L$, and integers K and L are relative prime:

$$\begin{aligned}\bar{u}=&\frac{\beta_0-\alpha_0}{\Theta}\theta+\sum_{i=0}^{\infty}\alpha_i r^i\cos i\theta\\&+\sum_{j=0}^{\infty}\sum_{k=1}^{L-1}\frac{\beta_{Lj+k}-\alpha_{Lj+k}\cos(Lj+k)\Theta}{\sin(Lj+k)\Theta}r^{Lj+k}\sin(Lj+k)\theta\\&+\sum_{j=1}^{\infty}\frac{1}{\Theta}(\beta_{Lj}\cos Lj\Theta-\alpha_{Lj})\varphi_{Lj}(r,\theta).\end{aligned}$$

3. Harmonic solutions involving Neumann conditions

3.1. The case of the N–D type

Consider:

$$\Delta u=0,\ \text{in } S,\quad \frac{\partial u}{\partial n}|_{\theta=0}=\sum_{i=0}^{\infty}\alpha_i r^i,\quad u|_{\theta=\Theta}=\sum_{i=0}^{\infty}\beta_i r^i. \tag{3.1}$$

Let $u=\bar{u}+u_g$, where the general solutions are given by

$$u_g=\sum_{k=0}^{\infty}d_k r^{\sigma k}\cos\sigma_k\theta, \tag{3.2}$$

when $\sigma_k=(k+1/2)\pi/\Theta$. The particular solution $\bar{u}$ satisfies:

$$\Delta\bar{u}=0,\ \text{in } S,\quad \left.\frac{\partial\bar{u}}{\partial n}\right|_{\theta=0}=\sum_{i=0}^{\infty}\alpha_i r^i,\quad \bar{u}|_{\theta=\Theta}=\sum_{i=0}^{\infty}\beta_i r^i. \tag{3.3}$$

Define the functions

$$\begin{aligned}\Psi_i=&\Psi_i(r,\theta)\\=&\begin{cases}\dfrac{r^i\cos i\theta}{\cos i\Theta}, & \text{if } i\Theta\neq\left(k+\dfrac{1}{2}\right)\pi,\ k=0,1,\ldots\\ \dfrac{(-1)^{k+1}}{\Theta}\psi_i(r,\theta), & \text{if } i\Theta=\left(k+\dfrac{1}{2}\right)\pi \text{ for some } k,\end{cases}\end{aligned} \tag{3.4}$$

where $\psi_i(r,\theta)$ is given in (2.16). Hence:

$$\left.\frac{\partial\Psi_i}{\partial n}\right|_{\theta=0}=-\frac{\partial\Psi_i}{r\partial\theta}|_{\theta=0}=0,\ \Psi_i|_{\theta=\Theta}=r^i,\ \forall\, r>0, i=1,2,\ldots \tag{3.5}$$

Choose the following particular solutions to (3.3)

$$\bar{u}=\sum_{i=1}^{\infty}A_i r^i\sin i\theta+B_0+\sum_{i=1}^{\infty}B_i\Psi_i(r,\theta), \tag{3.6}$$

where A_i and B_i are the coefficients. When $\theta=0$ we have:

$$\sum_{i=0}^{\infty}\alpha_i r^i=\left.\frac{\partial\bar{u}}{\partial n}\right|_{\theta=0}=-\sum_{i=1}^{\infty}A_i i r^{i-1}.$$

Then:

$$A_i = -\frac{\alpha_{i-1}}{i}, \quad i = 1, 2, \ldots \tag{3.7}$$

Also when $\theta = \Theta$:

$$\sum_{i=1}^{\infty} \beta_i r^i = \bar{u}|_{\theta=0} = \sum_{i=1}^{\infty} A_i r^i \sin i\Theta + B_0 + \sum_{i=1}^{\infty} B_i r^i.$$

This gives:

$$B_0 = \beta_0, \quad B_i = \beta_i - A_i \sin i\Theta = \beta_i + \frac{\alpha_{i-1}}{i} \sin i\Theta, \ i = 1, 2, \ldots \tag{3.8}$$

Hence, we obtain from (3.6) to (3.9) the particular solutions:

$$\bar{u} = -\sum_{i=1}^{\infty} \frac{\alpha_{i-1}}{i} r^i \sin i\theta + \beta_0 + \sum_{i=1}^{\infty} \left(\beta_i + \frac{\alpha_{i-1}}{i} \sin i\Theta\right) \Psi_i(r, \theta). \tag{3.9}$$

Eq. (3.9) is explicit for computation, in particular for directly displaying the existence of the mild singularity $O(r^i \ln r)$, when $i\Theta = (K + 1/2)\pi$ and $\beta_i + (\alpha_{i-1}/i)\sin i\Theta \neq 0$.

Below, we also list the useful formulas of the particular solution for some special Θ from (3.9).

(1) When $\Theta = \pi/2$:

$$\bar{u} = -\sum_{i=1}^{\infty} \frac{\alpha_{i-1}}{i} r^i \sin i\theta + \sum_{j=0}^{\infty} \frac{2}{\pi} \left((-1)^{j+1} \beta_{2j+1} - \frac{\alpha_{2j}}{2j+1}\right) \psi_{2j+1}(r, \theta) + \sum_{j=0}^{\infty} (-1)^j \beta_{2j} r^{2j} \cos 2j\theta. \tag{3.10}$$

(2) When $\Theta = 3\pi/2$:

$$\bar{u} = -\sum_{i=1}^{\infty} \frac{\alpha_{i-1}}{i} r^i \sin i\theta + \sum_{j=0}^{\infty} \frac{2}{3\pi} \left((-1)^j \beta_{2j+1} - \frac{\alpha_{2j}}{2j+1}\right) \psi_{2j+1}(r, \theta) + \sum_{j=0}^{\infty} (-1)^j \beta_{2j} r^{2j} \cos 2j\theta. \tag{3.11}$$

In Volkov [12], there are the different but equivalent formulas of (3.9). The discussions and comparisons between (3.9) and Volkov's are similar as the above.

3.2. The case of the D–N type

Now, we consider the mixed type of the D–N type:

$$\Delta u = 0, \ \text{in } S, \quad u|_{\theta=0} = \sum_{i=0}^{\infty} \alpha_i r^i, \quad \left.\frac{\partial u}{\partial n}\right|_{\theta=\Theta} = \sum_{i=0}^{\infty} \beta_i r^i. \tag{3.12}$$

Its solution is just the reflection of the solution of the N-D type about $\theta = \Theta/2$ with α_i and β_i switched. But for the completeness, we also include its derivation here. Let $u = \bar{u} + u_g$. We have the general solutions:

$$u_g = \sum_{k=0}^{\infty} d_k r^{\sigma_k} \sin(\sigma_k \theta), \quad \sigma_k = \frac{\left(k + \frac{1}{2}\right)}{\Theta} \pi. \tag{3.13}$$

The particular solution satisfies:

$$\Delta \bar{u} = 0, \ \text{in } S, \quad \bar{u}|_{\theta=0} = \sum_{i=0}^{\infty} \alpha_i r^i, \quad \frac{\partial \bar{u}}{\partial n}|_{\theta=\Theta} = \sum_{i=0}^{\infty} \beta_i r^i. \tag{3.14}$$

Define the functions:

$$\hat{\Phi}_i = \hat{\Phi}_i(r, \theta) = \begin{cases} \dfrac{r^i \sin i\theta}{i \cos i\Theta}, & \text{if } i\Theta \neq \left(k + \dfrac{1}{2}\right)\pi, \ k = 1, 2, \ldots \\ \dfrac{(-1)^{k+1}}{i\Theta} \varphi_i(r, \theta), & \text{if } i\Theta = \left(k + \dfrac{1}{2}\right)\pi \ \text{for some } k. \end{cases} \tag{3.15}$$

Hence:

$$\hat{\Phi}_i|_{\theta=0} = 0, \ \left.\frac{\partial \hat{\Phi}_i}{\partial n}\right|_{\theta=\Theta} = \frac{\partial \hat{\Phi}_i}{r\partial\theta}|_{\theta=\Theta} = r^{i-1}, \ \forall r > 0, i = 1, 2, \ldots \tag{3.16}$$

Choose the particular solutions to (3.14):

$$\bar{u} = \sum_{i=0}^{\infty} A_i r^i \cos i\theta + \sum_{i=1}^{\infty} B_i \hat{\Phi}_i(r, \theta), \tag{3.17}$$

where A_i and B_i are the coefficients. When $\theta = 0$ we have $A_i = \alpha_i$, and when $\theta = \Theta$

$$\sum_{i=0}^{\infty} \beta_i r^i = \left.\frac{\partial \bar{u}}{\partial n}\right|_{\theta=\Theta} = -\sum_{i=1}^{\infty} A_i r^{i-1} i \sin i\Theta + \sum_{i=1}^{\infty} B_i r^{i-1}.$$

This gives:

$$B_i = \beta_{i-1} + i\alpha_i \sin i\Theta. \tag{3.18}$$

Hence we obtain from the particular solutions (3.17):

$$\bar{u} = \sum_{i=0}^{\infty} \alpha_i r^i \cos i\theta + \sum_{i=1}^{\infty} (\beta_{i-1} + i\alpha_i \sin i\Theta) \hat{\Phi}_i(r, \theta). \tag{3.19}$$

Below, we also list the useful formulas from (3.19).

(1) When $\Theta=\pi/2$:

$$\bar{u} = \sum_{i=0}^{\infty} \alpha_i r^i \cos i\theta + \sum_{j=0}^{\infty} \frac{2}{\pi} \left((-1)^{j+1} \frac{\beta_{2j}}{2j+1} - \alpha_{2j+1} \right) \varphi_{2j+1}(r,\theta) + \sum_{j=1}^{\infty} (-1)^j \frac{\beta_{2j-1}}{2j} r^{2j} \sin 2j\theta. \tag{3.20}$$

(2) When $\Theta=3\pi/2$,

$$\bar{u} = \sum_{i=0}^{\infty} \alpha_i r^i \cos i\theta + \sum_{j=0}^{\infty} \frac{2}{3\pi} \left((-1)^{j} \frac{\beta_{2j}}{2j+1} - \alpha_{2j+1} \right) \varphi_{2j+1}(r,\theta) + \sum_{j=1}^{\infty} (-1)^j \frac{\beta_{2j-1}}{2j} r^{2j} \sin 2j\theta. \tag{3.21}$$

3.3. The case of the N–N type

Consider:

$$\Delta u = 0, \quad \text{in } S, \tag{3.22}$$

$$\left.\frac{\partial u}{\partial n}\right|_{\theta=0} = \sum_{i=0}^{\infty} \alpha_i r^i, \quad \left.\frac{\partial u}{\partial n}\right|_{\theta=\Theta} = \sum_{i=0}^{\infty} \beta_i r^i. \tag{3.23}$$

Let $u=\bar{u}+u_g$, where $u_g=\sum_{i=0}^{\infty} r^{\sigma_i}\cos\sigma_i\theta$, $\sigma_i=i\pi/\Theta$. The particular solution satisfies:

$$\Delta \bar{u} = 0, \quad \text{in } S, \tag{3.24}$$

$$\left.\frac{\partial \bar{u}}{\partial n}\right|_{\theta=0} = \sum_{i=0}^{\infty} \alpha_i r^i, \quad \left.\frac{\partial \bar{u}}{\partial n}\right|_{\theta=\Theta} = \sum_{i=0}^{\infty} \beta_i r^i. \tag{3.25}$$

Define the functions:

$$\hat{\Psi}_i = \hat{\Psi}_i(r,\theta) = \begin{cases} \dfrac{-r^i \cos i\theta}{i \sin i\Theta}, & \text{if } i\Theta \neq k\pi, \ \ k=1,2,\ldots \\ \dfrac{(-1)^{k+1}}{i\Theta}\psi_i(r,\theta), & \text{if } i\Theta = k\pi \text{ for some } k. \end{cases} \tag{3.26}$$

Hence:

$$\left.\frac{\partial \hat{\Psi}_i}{\partial n}\right|_{\theta=0} = 0, \quad \left.\frac{\partial \hat{\Psi}_i}{\partial n}\right|_{\theta=\Theta} = r^{i-1}, \quad \forall\, r>0,\ i=1,2,\ldots \tag{3.27}$$

Choose the particular solutions

$$\bar{u} = \sum_{i=1}^{\infty} A_i r^i \sin i\theta + \sum_{i=1}^{\infty} B_i \hat{\Psi}_i(r,\theta), \tag{3.28}$$

with the coefficients A_i and B_i. When $\theta=0$ we have:

$$\sum_{i=0}^{\infty} \alpha_i r^i = \frac{\partial \bar{u}}{\partial n}|_{\theta=0} = -\frac{\partial \bar{u}}{r\partial\theta}|_{\theta=0} = -\sum_{i=1}^{\infty} A_i i r^{i-1}.$$

Then $A_i=-\alpha_{i-1}/i$, i=1,2,…. Next, when $\theta=\Theta$:

$$\sum_{i=0}^{\infty} \beta_i r^i = \left.\frac{\partial \bar{u}}{\partial n}\right|_{\theta=\Theta} = \frac{\partial \bar{u}}{r\partial\theta}|_{\theta=\Theta} = \sum_{i=0}^{\infty} A_i r^{i-1} i \cos i\Theta + \sum_{i=0}^{\infty} B_i r^{i-1}.$$

This gives:

$$B_i = \beta_{i-1} + \alpha_{i-1}\cos i\Theta, \quad i=1,2,\ldots \tag{3.29}$$

Hence we obtain from (3.24) and (3.25) the particular solutions:

$$\bar{u} = -\sum_{i=1}^{\infty} \frac{\alpha_{i-1}}{i} r^i \sin i\theta + \sum_{i=1}^{\infty} (\beta_{i-1} + \alpha_{i-1}\cos i\Theta)\hat{\Psi}_i(r,\theta). \tag{3.30}$$

From (3.30), we also list the useful formulas for special angles Θ.

(1) When $\Theta=\pi$:

$$\bar{u} = -\sum_{i=1}^{\infty} \frac{\alpha_{i-1}}{i} r^i \sin i\theta + \sum_{i=1}^{\infty} \frac{1}{i\pi}((-1)^{i+1}\beta_{i-1} - \alpha_{i-1})\psi_i(r,\theta). \tag{3.31}$$

(2) When $\Theta=2\pi$:

$$\bar{u} = -\sum_{i=1}^{\infty} \frac{\alpha_{i-1}}{i} r^i \sin i\theta - \sum_{i=1}^{\infty} \frac{1}{2i\pi}(\beta_{i-1} + \alpha_{i-1})\psi_i(r,\theta). \tag{3.32}$$

(3) When $\Theta=\pi/2$:

$$\bar{u} = -\sum_{i=1}^{\infty}\frac{\alpha_{i-1}}{i}r^i\sin i\theta + \sum_{j=0}^{\infty}(-1)^{j+1}\frac{\beta_{2j}}{2j+1}r^{2j+1} \times\cos(2j+1)\theta + \sum_{j=1}^{\infty}\frac{1}{j\pi}((-1)^{j+1}\beta_{2j-1}-\alpha_{2j-1})\psi_{2j}(r,\theta). \quad (3.33)$$

(4) When $\Theta=3\pi/2$:

$$\bar{u} = -\sum_{i=1}^{\infty}\frac{\alpha_{i-1}}{i}r^i\sin i\theta + \sum_{i=0}^{\infty}(-1)^{j}\frac{\beta_{2j}}{2j+1}r^{2j+1} \times\cos(2j+1)\theta + \sum_{j=0}^{\infty}\frac{1}{3j\pi}((-1)^{j+1}\beta_{2j-1}-\alpha_{2j-1})\psi_{2j}(r,\theta). \quad (3.34)$$

Interestingly, when $\Theta=\pi/2$, π, $3\pi/2$ and 2π, for the N–D, the D–N and the N–N types, the worst singularity of $\bar{u}$ is $O(r\ln r)$, and for the D–D type, the worst singularity of $\bar{u}$ is $O(\theta/\Theta)$.

4. Extensions and analysis on singularity

4.1. Particular solutions for Poisson's equations

In this section, we consider the simple case of the Poisson equation

$$-\Delta\bar{u} = f, \quad \text{in } S, \quad (4.1)$$

$$\bar{u}|_{\Gamma_D} = g_D, \quad \frac{\partial\bar{u}}{\partial n}|_{\Gamma_N} = g_N, \quad (4.2)$$

where $\partial S=\Gamma=\Gamma_D\cup\Gamma_N$, $f=ax^iy^j$, $i,j=0,1,\ldots$, and a is a constant. Suppose that $i\geq j$ without loss of generality.

Case I. For $0\leq j\leq 1$:

$$\bar{u} = -a\frac{x^{i+2}y^j}{(i+1)(i+2)}.$$

Case II. For $2\leq j\leq 3$:

$$\bar{u} = -a\left\{\frac{x^{i+2}y^j}{(i+1)(i+2)} - \frac{x^{i+4}y^{j-2}j(j-1)}{(i+4)(i+3)(i+2)(i+1)}\right\}.$$

Case III. For $2k\leq j\leq 2k+1$, $k=1,2,\ldots$

$$\bar{u} = -a\frac{x^{i+2}y^j}{(i+1)(i+2)} - \frac{a}{(i+1)(i+2)} \times\sum_{\ell=1}^{k}(-1)^{\ell}b_{i,j,\ell}x^{i+2+2\ell}y^{j-2\ell},$$

where the coefficients:

$$b_{i,j,\ell} = \prod_{m=1}^{\ell}\frac{(j-2m)(j-2m-1)}{(i+2+2m)(i+1+2m)}.$$

Besides, Cheng et al. [3] gives a different approach for deriving the particular solution for the same function f. The particular solution is given as follow

$$\bar{u} = \begin{cases} \sum_{k=1}^{\text{Int}\left[\frac{j+2}{2}\right]} a(-1)^{k+1}\frac{i!j!x^{i+2k}y^{j-2k+2}}{(i+2k)!(j-2k+2)!}, & \text{for } i\geq j, \\ \sum_{k=1}^{\text{Int}\left[\frac{i+2}{2}\right]} a(-1)^{k+1}\frac{i!j!x^{i-2k+2}y^{j+2k}}{(i-2k+2)!(j+2k)!}, & \text{for } i<j, \end{cases}$$

where Int[s] means the integer part of s. By the above arguments and principle of superposition, we can obtain the particular solutions $\bar{u}$ for:

$$-\Delta\bar{u} = f = \sum_{i=0}^{M}\sum_{j=0}^{N}a_{ij}x^iy^j. \quad (4.3)$$

To find the solution of (4.1) and (4.2), it suffices to seek $\bar{v}=u-\bar{u}$ to satisfy (4.1) and (4.2):

$$\Delta\bar{v} = 0, \text{ in } S, \quad (4.4)$$

$$\bar{v} = g_D - \bar{u}, \text{ on } \Gamma_D, \quad (4.5)$$

$$\frac{\partial\bar{v}}{\partial n} = g_N - \frac{\partial\bar{u}}{\partial n}, \text{ on } \Gamma_N.$$

Hence, it is reduced to the Laplace equation with the Dirichlet–Neumann conditions, which solutions have been provided in Sections 2 and 3.

4.2. Extensions to not smooth functions of g_D and g_N

In this subsection, we consider that the functions g_D and g_N are not smooth. First, consider the D–D type

$$\Delta\bar{u} = 0, \text{ in } S, \quad \bar{u}|_{\theta=0} = ar^q, \quad \bar{u}|_{\theta=\Theta} = br^p, \quad (4.6)$$

where p and q are real. For the Laplace solutions $u\in H^1(S)$, where $H^k(S)$ is the Sobolev space, the boundary functions of the Dirichlet and the Neumann conditions satisfy $g_D\in H^{1/2}(\Gamma_D)$ and $g_N\in H^{-1/2}(\Gamma_N)$ (see Babuska [1]). Hence we assume $p,q>-1/2$ in (4.6).

Hence p and q are not confined to be positive integers (cf. Sections 2 and 3). When $p\Theta$, $q\Theta\neq\pm k\pi$. The particular solutions are given by:

$$\bar{u} = br^p\frac{\sin p\theta}{\sin p\Theta} + ar^q\frac{\sin q(\Theta-\theta)}{\sin q\Theta}. \quad (4.7)$$

For simplicity, here we only give one term on the right hand side of the Dirichlet condition (4.6). For more terms,

the particular solutions can be obtained easily by linear superposition as done in Sections 2 and 3. Since the solutions $O(r^p \ln r)$ for $p \in (-1/2,1)$ are of strong singularity, we use the formulas in symmetric form of (2.23) as those in Volkov [12].

Suppose that $p\Theta = \pm m\pi$ and $q\Theta = \pm \ell\pi$, where m and ℓ are positive integers. The particular solutions are given by:

$$\bar{u} = \frac{b}{\Theta}\frac{\varphi_p(r,\theta)}{\cos p\Theta} + \frac{a}{\Theta}\frac{\varphi_q(r,\Theta-\theta)}{\cos q\Theta} = \frac{(-1)^m b}{\Theta}\varphi_p(r,\theta) + \frac{(-1)^\ell a}{\Theta}\varphi_q(r,\Theta-\theta). \tag{4.8}$$

When $p\Theta \neq \pm m\pi$ and $q\Theta \neq \pm \ell\pi$, the particular solutions can be easily obtained. Moreover, the function $\varphi_q(r, \Theta-\theta)$ is defined in (2.13), and may be further simplified (see Sections 2 and 3).

Next, consider the N–D type

$$\Delta\bar{u} = 0, \ \text{in } S, \quad \frac{\partial\bar{u}}{\partial n}|_{\theta=0} = ar^q, \quad \bar{u}|_{\theta-\Theta} = br^p, \tag{4.9}$$

where real number $p > -1/2$ and $q > -3/2$. For $p\Theta$, $(q+1)\Theta \neq \pm(k+1/2)\pi$, the particular solutions are:

$$\bar{u} = br^p\frac{\cos p\theta}{\cos p\Theta} + \frac{a}{q+1}r^{q+1}\frac{\sin(q+1)(\Theta-\theta)}{\cos(q+1)\Theta}. \tag{4.10}$$

For $p\Theta = \pm(m+1/2)\pi$, $(q+1)\Theta = \pm(\ell+1/2)\pi$, m and ℓ are positive integers, the particular solutions

$$\bar{u} = -\frac{b}{\Theta}\frac{\psi_p(r,\theta)}{\sin p\Theta} - \frac{a}{(q+1)\Theta}\frac{\varphi_{q+1}(r,\Theta-\theta)}{\sin(q+1)\Theta} = -\frac{\pm(-1)^m b}{\Theta}\psi_p(r,\theta) - \frac{\pm(-1)^\ell a}{(q+1)\Theta}\varphi_q(r,\Theta-\theta), \tag{4.11}$$

where $\psi_p(r,\theta)$ is defined in (2.14). The particular solutions of the D–N type can be obtained from those of the N–D type by $\varphi = \Theta - \theta$.

Finally, we consider the N–N type

$$\Delta\bar{u} = 0, \ \text{in } S, \quad \left.\frac{\partial\bar{u}}{\partial n}\right|_{\theta=0} = ar^q, \quad \frac{\partial\bar{u}}{\partial n}|_{\theta=\Theta} = br^p, \tag{4.12}$$

where real $p,q > -3/2$. When $(p+1)\Theta$ and $(q+1)\Theta \neq \pm k\pi$, $k = 0,1,\ldots$, the particular solutions are:

$$\bar{u} = -\frac{b}{p+1}r^{p+1}\frac{\cos(p+1)\theta}{\sin(p+1)\Theta} + \frac{a}{q+1}r^{q+1}\frac{\cos(q+1)(\Theta-\theta)}{\sin(q+1)\Theta}. \tag{4.13}$$

When $(p+1)\Theta = \pm m\pi$, $(q+1)\Theta = \pm \ell\pi$, m, $\ell = 1,2,\ldots$, the particular solutions are:

$$\bar{u} = -\frac{b}{(p+1)\Theta}\frac{\psi_{p+1}(r,\theta)}{\cos(p+1)\Theta} + \frac{a}{(q+1)\Theta}\frac{\psi_{q+1}(r,\Theta-\theta)}{\cos(q+1)\Theta} = -\frac{(-1)^m b}{(p+1)\Theta}\psi_{p+1}(r,\theta) - \frac{(-1)^\ell a}{(q+1)\Theta}\psi_{q+1} \quad (r,\Theta-\theta). \tag{4.14}$$

Of course, we may derive the particular solutions for $\Theta = \pi/2$, $3\pi/2$, 2π and 2π by following Sections 2 and 3.

4.3. Regularity and singularity of the solutions of $\Theta = \pi/2$, $3\pi/2$, π, 2π

From the analysis in Sections 2 and 3, when g_D and g_N are highly smooth on ∂S, the solutions u inside of S may also be smooth for $\Theta = \pi/2$, π. However, the solution u near the corners may have the mild singularities $O(r^k \ln r)$, $k = 1,2,\ldots$ in addition to the strong singularities. Since the singularity analysis on general solutions can be found in textbooks (cf. Li [5]), we focus on the analysis for the particular solution $\bar{u}$. In particular, we consider when $\Theta = i\pi/2$, $i = 1$–4 which exist in Motz's and cracked beam problems [9], and the L-shaped domain problems and the general cracked domains in Fig. 5 (see [5,9]).

4.3.1. For the Case of $\Theta = \pi/2$

First, consider a simple case of the D–D type as $\Theta = \pi/2$

$$\Delta\bar{u} = 0, \ \text{in } S, \quad \bar{u} = \alpha_0 + \alpha_1 r + \alpha_2 r^2, \qquad \theta = 0, \quad \bar{u} = \beta_0 + \beta_1 r + \beta_2 r^2, \ \ \theta = \Theta, \tag{4.15}$$

where α_i and β_i are constants. Only the quadratic polynomials in the Dirichlet conditions are chosen, because the resulted singularities are strongest among all mild singularity.

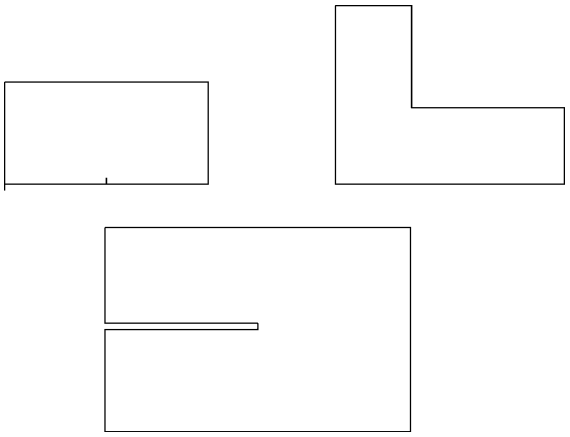

Fig. 5. The popular domains in testing models with $\Theta = i\pi/2$, $i = 1$–4.

We then obtain from (2.36):

$$\bar{u} = \alpha_0 + \frac{\beta_0 - \alpha_0}{\Theta}\theta + \beta_1 r \sin\theta - \frac{\beta_2 + \alpha_2}{\Theta}\varphi_2(r,\theta) + \alpha_1 r\cos\theta + \alpha_2 r^2\cos 2\theta. \quad (4.16)$$

In (4.16), when $\beta_0 \neq \alpha_0$, the function $\theta \notin H^1(S)$, called the discontinuity singularity. Moreover, when $\beta_2+\alpha_2 \neq 0$, the function $r^2 \ln r \notin H^3(S)$, called a mild singularity, compared with the crack singularity

$$u = \mathrm{O}\left(r^{1/2}\right) \notin H^2(S),$$

in the cracked beam problem. Interestingly, the case of $\beta_2+\alpha_2 \neq 0$ implies $u_{xx}+u_{yy}=\beta_2+\alpha_2 \neq 0$ against the Laplace equation. Note that the case of β_1 or α_1 has no effect on singularities because $r\sin\theta = y$ and $r\cos\theta = x$. In Section 5, Model II of crack plus mild singularities will be designed on the rectangles with $\Theta = \pi/2$.

Next, consider the N–D type:

$$\Delta\bar{u} = 0, \ \text{in } S, \quad \frac{\partial \bar{u}}{\partial n} = \alpha_0 + \alpha_1 r + \alpha_2 r^2, \qquad \theta = 0, \quad \bar{u} = \beta_0 + \beta_1 r + \beta_2 r^2, \ \ \theta = \Theta. \quad (4.17)$$

From (3.10) we obtain:

$$\bar{u} = \beta_0 - \frac{\beta_1 + \alpha_0}{\Theta}\psi_1(r,\theta) - \beta_2 r^2\cos 2\theta - \alpha_0 r\sin\theta - \frac{\alpha_1}{2}r^2\sin 2\theta - \frac{\alpha_2}{3}\left\{r^3\sin 3\theta + \frac{1}{\Theta}\psi_3(r,\theta)\right\}. \quad (4.18)$$

From (4.18), when $\beta_1+\alpha_0 \neq 0$ which results from:

$$\alpha_0 = \frac{\partial \bar{u}}{\partial n} = -\frac{\partial \bar{u}}{\partial y} \neq -\frac{\partial \bar{u}}{\partial r} = -\beta_1, \quad (4.19)$$

there exists a mild singularity $\mathrm{O}(r\ln r)$, and when $\alpha_2 \neq 0$, there exists $\mathrm{O}(r^3 \ln r)$. Interestingly, β_0, β_2 and α_1 do not cause any singularity in the N–D type, since $r^2\cos 2\theta = (x^2 - y^2)$ and $r\sin 2\theta = 2xy$.

The conclusion for the D–N type can be drawn similarly. Below we only consider the N–N type:

$$\Delta\bar{u} = 0, \ \text{in } S, \quad \frac{\partial \bar{u}}{\partial n} = \alpha_0 + \alpha_1 r + \alpha_2 r^2, \qquad \theta = 0, \quad \frac{\partial \bar{u}}{\partial n} = \beta_0 + \beta_1 r + \beta_2 r^2, \ \ \theta = \Theta. \quad (4.20)$$

From (3.33) we obtain:

$$\bar{u} = -\beta_0 r\cos\theta + \frac{\beta_1 - \alpha_1}{2\Theta}\psi_2(r,\theta) + \frac{\beta_2}{3}r^3\cos 3\theta - \alpha_0 r\sin\theta - \frac{\alpha_1}{2}r^2\sin 2\theta - \frac{\alpha_2}{3}r^3\sin 3\theta. \quad (4.21)$$

Table 1
The singularities for the particular solutions of the Dirichlet–Neumann conditions assigned by quadratic polynomials when $\Theta = \pi/2$

Types	Conditions	Singularity of $\bar{u}$	Not in $H^k(S)$
D–D	$\beta_0 \neq \alpha_0$	$\mathrm{O}(\theta/\Theta)$	$\notin H^1(S)$
	$\beta_2+\alpha_2 \neq 0$	$\mathrm{O}(r^2 \ln r)$	$\notin H^3(S)$
N–N	$\beta_1-\alpha_1 \neq 0$	$\mathrm{O}(r^2 \ln r)$	$\notin H^3(S)$
N–D	$\beta_1+\alpha_0 \neq 0$	$\mathrm{O}(r \ln r)$	$\notin H^2(S)$
	$\alpha_2 \neq 0$	$\mathrm{O}(r^3 \ln r)$	$\notin H^4(S)$

Only $\beta_1-\alpha_1 \neq 0$ resulting from $\bar{u}_{xy} \neq \bar{u}_{yx}$ will cause the singularity $\mathrm{O}(r^2 \ln r)$.

We summarize the singularities at the corner with $\Theta = \pi/2$ in Table 1. The discontinuity $\beta_0 \neq \alpha_0$ in the D–D type is the strongest. The next strongest singularity occurs in the N–D type of $\beta_1+\alpha_0 \neq 0$ and the N–N type of $\beta_1 \neq \alpha_1$.

4.3.2. For the case of $\Theta = \pi$

Next, we consider the D–D type of (4.15) with $\Theta = \pi$. From (2.34) we obtain:

$$\bar{u} = \alpha_0 + \frac{\beta_0 - \alpha_0}{\Theta}\theta + \alpha_1 r\cos\theta + \alpha_2 r^2\cos 2\theta - \frac{\beta_1 + \alpha_1}{\Theta}\varphi_1(r,\theta) + \frac{\beta_2 - \alpha_2}{\Theta}\varphi_2(r,\theta). \quad (4.22)$$

When $\beta_0 \neq \alpha_0$ the solution of $\mathrm{O}(\theta/\Theta)$ is discontinuity at origin O, and when $\beta_2 \neq \alpha_2$, the solutions of $\mathrm{O}(r^2 \ln r)$ are obtained. Note that the case of $\beta_1 \neq -\alpha_1$, will also cause the singularity of $\mathrm{O}(r \ln r)$. In fact, the case of $\beta_1 \neq -\alpha_1$, implies the existing of a piecewise x-function because $r = x$ at $\theta = 0$ but $r = -x$ at $\theta = \pi$.

Consider the N–N type of (4.20) with $\Theta = \pi$. From (3.31) for $\Theta = \pi$

$$\bar{u} = -\alpha_0 r\sin\theta - \frac{\alpha_1}{2}r^2\sin 2\theta - \frac{\alpha_2}{3}r^3\sin 3\theta + \frac{\beta_0 - \alpha_0}{\Theta}\varphi_1(r,\theta) - \frac{\beta_1 + \alpha_1}{2\Theta}\varphi_2(r,\theta) + \frac{\beta_2 - \alpha_2}{3\Theta}\varphi_3(r,\theta). \quad (4.23)$$

When $\beta_0 \neq \alpha_0$, $\beta_1 \neq -\alpha_1$, and $\beta_2 \neq \alpha_2$, there exist the solutions with $u = \mathrm{O}(\theta/\Theta)$, $\mathrm{O}(r\ln r)$ and $\mathrm{O}(r^3 \ln r)$, respectively.

Consider the N–D type of (4.17) with $\Theta = \pi$, which appears in Motz's and the cracked beam problems in [9]. The general solutions are

$$u_g = \sum_{i=0}^{L} d_i r^{i+1/2}\cos\left(i+\frac{1}{2}\right)\theta,$$

and the particular solutions are obtained from (3.9)

$$\bar{u} = \sum_{k=0}^{2}(-1)^k\beta_k r^k\cos k\theta - \sum_{k=1}^{3}\frac{\alpha_{k-1}}{k}r^k\sin k\theta. \quad (4.24)$$

Interestingly, the singularity results only from the general solutions of $O(r^{1/2})$, but not from $\beta_i \neq 0$ and $\alpha_i \neq 0$.

4.3.3. For the case of $\Theta = 3\pi/2$

The boundary angle $\Theta = 3\pi/2$ exists in a typical concave polygon, such as the L-shaped domains in Fig. 5. First, we consider the D–D type of (4.15) with $\Theta = 3\pi/2$. The solution is $u = \bar{u} + u_g$, where

$$u_g = \sum_{i=1}^{L} \mathrm{d}_i r^{(2/3)i} \sin\left(\frac{2i}{3}\right)\theta,$$

and the particular solutions from (2.37) are:

$$\bar{u} = \alpha_0 + \frac{\beta_0 - \alpha_0}{\Theta}\theta - \beta_1 r \sin\theta - \frac{\beta_2 + \alpha_2}{\Theta}\varphi_2(r,\theta) + \alpha_1 r \cos\theta + \alpha_2 r^2 \cos 2\theta. \quad (4.25)$$

Compared the above function with that of $\Theta = \pi/2$ in (4.16), only the sign in front of the term $\beta_1 r \sin\theta$ is different. Note that when $d_1 \neq 0$, $u_g = O(r^{2/3}) \notin H^2(S)$ is the next strongest singularity to that of $O(\theta/\Theta)$.

Consider the N–N type of (4.20) with $\Theta = 3\pi/2$. The general solutions are

$$u_g = \sum_{i=0}^{L} d_i r^{(2/3)i} \cos\left(\frac{2i}{3}\right)\theta,$$

and the particular solutions (3.34) give:

$$\bar{u} = \beta_0 r \cos\theta + \frac{\beta_1 - \alpha_1}{2\Theta}\psi_2(r,\theta) - \frac{\beta_2}{3} r^3 \cos 3\theta - \alpha_0 r \sin\theta - \frac{\alpha_1}{2} r^2 \sin 2\theta - \frac{\alpha_2}{3} r^3 \sin 3\theta. \quad (4.26)$$

Compared (4.26) with (4.21), only the signs in front of $\beta_0 r \cos\Theta$ and $(\beta_2/3) r^3 \cos 3\theta$ are different.

Finally, consider the N–D type of (4.17) with $\Theta = 3\pi/2$. The general solutions are $u_g = \sum_{i=0}^{L} \mathrm{d}_i r^{\sigma i} \cos(\sigma_i \theta)$ where $\sigma_i = (2/3)i + (1/3)$. The particular solutions of (3.11) give:

$$\bar{u} = \beta_0 + \frac{\beta_1 - \alpha_0}{\Theta}\psi_1(r,\theta) - \beta_2 r^2 \cos 2\theta - \alpha_0 r \sin\theta - \frac{\alpha_1}{2} r^2 \sin 2\theta - \frac{\alpha_2}{3}\left\{ r^3 \sin 3\theta + \frac{1}{\Theta}\psi_3(r,\theta)\right\}. \quad (4.27)$$

The strongest singularity of u is $O(r^{1/3})$.

4.3.4. For the case of $\Theta = 2\pi$

The boundary angle $\Theta = 2\pi$ occurs for the domains with an inside crack in Fig. 5. First, we consider the D–D type of (4.15) with $\Theta = 2\pi$. The general solutions are given by $u_g = \sum_{i=1}^{L} \mathrm{d}_i r^{i/2} \sin(i/2)\theta$, and the particular solutions from (2.35) are:

$$\bar{u} = \alpha_0 + \frac{\beta_0 - \alpha_0}{\Theta}\theta + \sum_{k=1}^{2} \alpha_k r^k \cos k\theta + \sum_{k=1}^{2} \frac{\beta_k - \alpha_k}{\Theta}\varphi_k(r,\theta). \quad (4.28)$$

When $\beta_0 \neq \alpha_0$ the singularity $O(\theta/\Theta)$ is the strongest. The next strongest singularity results from $u_g = O(r^{1/2})$. Also when $\beta_i \neq \alpha_i$, $i = 1,2$, the mild singularities $O(r_1 \ln r)$ occur.

Consider the N–N type of (4.20) with $\Theta = 2\pi$. The general solutions are $u_g = \sum_{i=0}^{L} \mathrm{d}_i r^{1/2} \cos(i/2)\theta$, where d_0 is an arbitrary constant, and the particular solutions from (3.32) give:

$$\bar{u} = -\sum_{k=1}^{3} \frac{\alpha_{k-1} + \beta_{k-1}}{k\Theta}\psi_k(r,\theta) - \sum_{k=1}^{3} \frac{\alpha_{k-1}}{k} r^k \sin k\theta. \quad (4.29)$$

Consider the N–D type of (4.17) with $\Theta = 2\pi$, $u_g = \sum_{i=0}^{L} \mathrm{d}_i r^{\sigma i} \cos(\sigma_i \theta)$, where $\sigma_i = i/2 + 1/4$. The particular solutions from (3.9) are:

$$\bar{u} = \sum_{k=0}^{2} \beta_k r^k \cos k\theta - \sum_{k=1}^{3} \frac{\alpha_{k-1}}{k} r^k \sin k\theta. \quad (4.30)$$

Tables 2–4 list the overviews of the singularities of particular solutions for $\Theta = 3\pi/2$, π, 2π.

Among all cases of $\Theta = \pi/2$, $3\pi/2$, π, 2π, the strongest singularity is still $O(\theta/\Theta)$, and the next strong one $O(r^{1/4})$ results from the N–D type of $\Theta = 2\pi$. Based on the analysis for the harmonic functions on the polygonal domains, we understand completely the regularity and singularity of Laplace's solutions. Therefore, we may deliberately design the brand-new models of different kinds of singularities. In this paper, we consider the test models on the simplest

Table 2
The singularities for the general and the particular solutions for the Dirichlet–Neumann conditions assigned by quadratic polynomials when $\Theta = \pi$

Types	Conditions	Singularity of $\bar{u}$	Singularity of u_g
D–D	$\beta_0 \neq \alpha_0$	$O(\theta/\Theta)$	/
	$\beta_1 + \alpha_1 \neq 0$	$O(r \ln r)$	/
	$\beta_2 \neq \alpha_2$	$O(r^2 \ln r)$	/
N–N	$\beta_0 \neq \alpha_0$	$O(r \ln r)$	/
	$\beta_1 + \alpha_1 \neq 0$	$O(r^2 \ln r)$	/
	$\beta_2 \neq \alpha_2$	$O(r^3 \ln r)$	/
N–D	/	/	$O(r^{1/2})$

Table 3
The singularities for the general and the particular solutions for the Dirichlet–Neumann conditions assigned by quadratic polynomials when $\Theta = 3\pi/2$

Types	Conditions	Singularity of $\bar{u}$	Singularity of u_g
D–D	$\beta_0 \neq \alpha_0$	$O(\theta/\Theta)$	$O(r^{2/3})$
	$\beta_2 + \alpha_2 \neq 0$	$O(r^2 \ln r)$	$O(r^{2/3})$
N–N	$\beta_1 - \alpha_1 \neq 0$	$O(r^2 \ln r)$	$O(r^{2/3})$
N–D	$\beta_1 \neq \alpha_0$	$O(r \ln r)$	$O(r^{1/3})$
	$\alpha_2 \neq 0$	$O(r^3 \ln r)$	$O(r^{1/3})$

Table 4
The singularities for the general and the particular solutions for the Dirichlet–Neumann conditions assigned by quadratic polynomials when $\Theta=2\pi$

Types	Conditions	Singularity of $\bar{u}$	Singularity of u_g
D–D	$\beta_0\neq\alpha_0$	$O(\theta/\Theta)$	$O(r^{1/2})$
	$\beta_1\neq\alpha_1$	$O(r\ln r)$	$O(r^{1/2})$
	$\beta_2\neq\alpha_2$	$O(r^2\ln r)$	$O(r^{1/2})$
N–N	$\beta_0+\alpha_0\neq0$	$O(r\ln r)$	$O(r^{1/2})$
	$\beta_1+\alpha_1\neq0$	$O(r^2\ln r)$	$O(r^{1/2})$
	$\beta_2+\alpha_2\neq0$	$O(r^3\ln r)$	$O(r^{1/2})$
N–D	/	/	$O(r^{1/4})$

rectangular domain in Fig. 5, and employ the particular solutions in Section 4.3.1. Of course, we may also design other testing models on the L-shaped and the inside cracked domains as shown in Fig. 5, by means of results in Sections 4.3.2–4.3.4.

5. New models of singularities for Laplace's equation

5.1. Two models

The singularity models play an important role in studying numerical methods, because one may compare their performance for the same models. Two popular models, Motz's and the cracked beam problems, have been explored in Lu et al [9]. In this paper, we propose a new discontinuity model, called Model I (see Fig. 6)

$$\begin{aligned}&\Delta u=0,\ \text{ in } S,\quad u=0,\ \text{ on } \bar{OD},\\ &u=500,\ \text{ on } \bar{OA}\cup\bar{AB},\quad \frac{\partial u}{\partial n}=0,\ \text{ on } \bar{BC}\cup\bar{CD},\end{aligned}\tag{5.1}$$

where $S=\{(x,y)|-1<x<1,\ 0<y<1\}$.

Note that Models I is different from the Motz's problem only on the boundary condition on $\bar{OA}$, where the Dirichlet condition $u=500$ is used to replace the Neumann condition $\partial u/\partial n=0$. The solution u at the origin is discontinuous, having much stronger singularity than that of Motz's

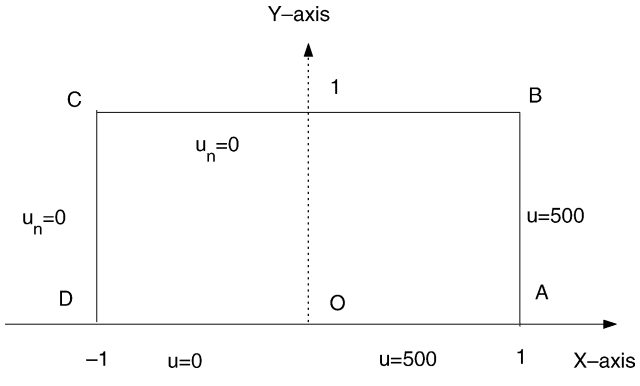

Fig. 6. Model I.

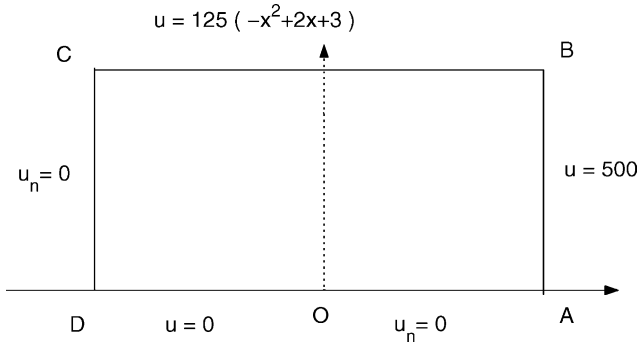

Fig. 7. Model II.

problem. We have the solution expansion from (4.22)

$$v=\frac{500(\pi-\theta)}{\pi}+\sum_{i=1}^{L}c_i r^i\sin i\theta,\tag{5.2}$$

where c_i are the unknown coefficients to be sought. Since the function (5.2) also satisfies the boundary conditions on $\bar{DO}$ and $\bar{OA}$ already, then c_i can be found to satisfy the rest boundary conditions on ∂S as best as possible. We will choose the collocation Trefftz method described in Section 5.2 to solve it.

Consider the following model of the crack plus mild singularities of $\rho^k\ln\rho$, $k=1,2$, which are developed from Motz's problem, called Model II (see Fig. 7):

$$\begin{aligned}&\Delta u=0,\ \text{ in } S,\quad u=0,\ \text{ on } \bar{OD},\\ &u=500,\ \text{ on } \bar{AB},\quad \frac{\partial u}{\partial n}=0,\ \text{ on } \bar{OA}\cup\bar{CD},\\ &u=125(-x^2+2x+3),\ \text{ on } \bar{BC}.\end{aligned}\tag{5.3}$$

Since the function on $\bar{BC}$ is expressed by

$$\begin{aligned}u&=500(x+1)-125(x+1)^2\\ &=500-125(x-1)^2,\ \text{ on } \bar{BC},\end{aligned}\tag{5.4}$$

we obtain the solutions at the corners B and C

$$\begin{aligned}v_1&=\bar{v}_1+\sum_{i=1}^{M}a_i\rho^{2i}\sin 2i\phi,\ \text{ in } S_1,\\ v_2&=\bar{v}_2+\sum_{i=1}^{M}b_i\xi^{2i+1}\sin(2i+1)\eta,\ \text{ in } S_2,\end{aligned}\tag{5.5}$$

where the coefficients a_i and b_i are unknowns, (ρ,ϕ) and (ξ,η) are the polar coordinates at corners B and C, respectively, and S_1 and S_2 are the subdomains (see Fig. 8):

$$S_1=\left\{(\rho,\phi)|0\le\rho\le\rho_1,\ 0\le\phi\le\frac{\pi}{2}\right\},$$

$$S_2=\left\{(\xi,\eta)|0\le\xi\le\xi_1,\ 0\le\eta\le\frac{\pi}{2}\right\}.$$

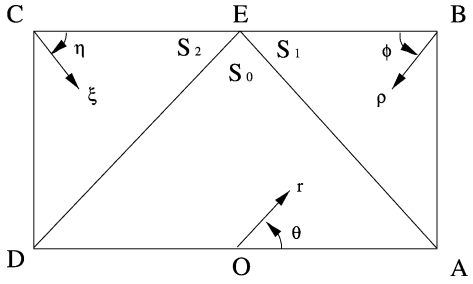

Fig. 8. Partition of the rectangle.

The functions $\bar{v}_1$ and $\bar{v}_2$ can be found by following the particular solutions in Section 4.3

$$\bar{v}_1 = 500 - 125\rho^2\cos 2\phi + \frac{125}{\Theta}\rho^2(\ln\rho\sin 2\phi + \phi\cos 2\phi),$$
$$\bar{v}_2 = -125\xi^2\cos 2\eta + 500\xi\cos\eta - \frac{500}{\Theta}\xi(\ln\xi\sin\eta + \eta\cos\eta). \tag{5.6}$$

where $\Theta = \pi/2$.

Let $S = S_0 \cup S_1 \cup S_2$ shown in Fig. 8. Hence, the piecewise admissible functions are given by:

$$v = \begin{cases} v_0 = \sum_{i=0}^{L} d_i r^{i+(1/2)} \cos\left(i + \frac{1}{2}\right)\theta, & \text{in } S_0, \\ v_1 = \bar{v}_1 + \sum_{i=1}^{M} a_i \rho^{2i} \sin 2i\phi, & \text{in } S_1, \\ v_2 = \bar{v}_2 + \sum_{i=0}^{N} b_i \xi^{2i+1} \sin(2i+1)\eta, & \text{in } S_2. \end{cases} \tag{5.7}$$

Note that the solutions at corners B and C have the mild singularities, $O(\rho^2 \ln \rho)$ and $O(\xi \ln \xi)$, respectively.

5.2. The Trefftz method

Based on the above analysis, we have found the local particular solutions near all the corners of S. If there exist the singularities, e.g. the discontinuity as $O(\theta/\Theta)$, the angular singularity as $O(r^p)$, $0 < p < 1$, and the mild singularity as $O(r^k \ln r)$, $k = 1,2,\ldots$, we may split S by a interface Γ_0 into finite sub-polygons S_i, e.g. $S = \cup_{i=0}^{N} S_i$. In each S_i, there exists only one singularity point at one exterior corner (see Fig. 9). We denote simply

$$v = v_i = \bar{v}_i + \sum_{k=0}^{N_i} c_k^{(i)} H_k^{(i)}, \quad \text{in } S_i, \tag{5.8}$$

where $\bar{v}_i$ are the particular solutions, $H_k^{(i)}$ are the known functions satisfying the Laplace equation, and $c_k^{(i)}$ are the unknown coefficients. Inside S_0 in Fig. 9, the smooth

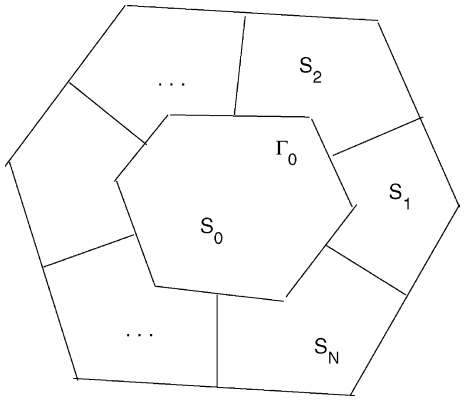

Fig. 9. Partition for the collocation Trefftz method.

solutions can be expressed by

$$u = \sum_{i=0}^{\infty} a_i r^i \cos i\theta + \sum_{i=1}^{\infty} b_i r^i \sin i\theta,$$

where a_i and b_i are coefficients.

Suppose that the piecewise admissible functions (5.8) satisfy (4.1) in S_i and the exterior Dirichlet–Neumann conditions. Then the coefficients $c_k = c_k^{(i)}$ may be sought by satisfying the interior continuity conditions:

$$u^+ = u^-, \quad \frac{\partial u^+}{\partial n} = \frac{\partial u^-}{\partial n}, \quad \text{on } \Gamma_0. \tag{5.9}$$

Define the errors on Γ_0

$$\|v\|_B = \left\{ \int_{\Gamma_0} (v^+ - v^-)^2 d\ell + w^2 \int_{\Gamma_0} \left(\frac{\partial v^+}{\partial n} - \frac{\partial v^-}{\partial n} \right)^2 d\ell \right\}^{1/2}, \tag{5.10}$$

where w is a suitable weight. For Model II, we choose $w = \min\{1/L+1, 1/2M, 1/2N+1\}$ (see [5]). Then the coefficients $\tilde{c}_k = \tilde{c}_k^{(i)}$ are found by

$$I(\tilde{c}_k) = \min_{c_k} I(c_k), \tag{5.11}$$

where:

$$I(c_k) = \|v\|_B^2 = \int_{\Gamma_0} (v^+ - v^-)^2 d\ell + w^2 \int_{\Gamma_0} \left(\frac{\partial v^+}{\partial n} - \frac{\partial v^-}{\partial n} \right)^2 d\ell. \tag{5.12}$$

Eq. (5.11) is called the Trefftz method. When the integrals in (5.12) involve numerical quadrature, we denote

$$\hat{I}(c_k) = \hat{\int}_{\Gamma_0} (v^+ - v^-)^2 d\ell + w^2 \hat{\int}_{\Gamma_0} \left(\frac{\partial v^+}{\partial n} - \frac{\partial v^-}{\partial n} \right)^2 d\ell, \tag{5.13}$$

where $\hat{\int}_{\Gamma_0}$ is evaluated by some rules. The collocation Trefftz method is to seek the coefficients $\hat{c}_k = \hat{c}_k^{(i)}$ by:

$$\hat{I}(\hat{c}_k) = \min_{c_k} \hat{I}(c_k). \tag{5.14}$$

The detailed algorithms and error analysis are also provided in Lu et al. [9]. The exponential convergence rates can be achieved if all corner singularities are taken into account.

5.3. Numerical experiments

First, consider Model I with discontinuity solutions. We divide $A\bar{B}$ by NNP uniform sections, and use the central rule for numerical integration. Based on our trial computation, choose NNP$=L$, and carry out the collocation Trefftz method. The error norms, condition numbers (*Cond.*) of the associated matrix, and the leading coefficient $\hat{c}_1$ are listed in Table 5, and the computed coefficients in Table 6. From Table 5, we can see:

$$\|\epsilon\|_B = \mathrm{O}((0.56)^L), \quad Cond. = \mathrm{O}((1.43)^L). \tag{5.15}$$

The coefficient $\hat{c}_1$ has 12 significant digits, if we compare the data in the last two rows in Table 5. From Table 6, the declining behavior of coefficients $\hat{c}_1$ is like that in Motz's problem, and the errors $\|\epsilon\|_{\mathrm{B}}$ in Table 5 decline by a factor about 0.1 by increasing four terms of series $\sin i\theta$ (see [9]).

The function $\hat{u} = 500(\pi - \theta)/\pi$ in (5.2) satisfies $\hat{u} \notin H^1(S)$ but $\hat{u} \in H^{1/2}(S)$ only. This causes a dilemma for the error analysis of the Trefftz method for Model I. In fact, let $w = u - \hat{u}$. We obtain from (5.1):

$$\begin{aligned} &\Delta w = 0, \ \text{ in } S, \quad w = 0, \ \text{ on } A\bar{D}, \\ &w = 500 - \hat{u}, \ \text{ on } A\bar{B}, \\ &\frac{\partial w}{\partial n} = -\frac{\partial \hat{u}}{\partial n}, \ \text{ on } B\bar{C} \cup C\bar{D}. \end{aligned} \tag{5.16}$$

So the solution w is a smooth solution. Hence, we may also achieve the exponential convergence rates by the collocation Trefftz method for Model I (see [9]).

Table 5
The error norms, condition numbers and the leading coefficient from the collocation Trefftz method for Model I with discontinuity solutions

L	NNP	$\|\varepsilon\|_{\mathrm{B}}$	*Cond.*	$\hat{c}_1$
4	4	8.00	7.21	388.19237952022
8	8	0.374	39.4	431.70665114799
12	12	0.310(−1)	189	432.14376500110
16	16	0.262(−2)	865	432.14136607970
20	20	0.240(−3)	0.385(4)	432.14228064373
24	24	0.226(−4)	0.168(5)	432.14218726860
28	28	0.219(−5)	0.725(5)	432.14219772889
32	32	0.217(−6)	0.309(6)	432.14219655948
36	36	0.218(−7)	0.131(7)	432.14219669083
40	40	0.221(−8)	0.553(7)	432.14219667602
44	44	0.227(−9)	0.230(8)	432.14219667770
48	48	0.234(−10)	0.892(8)	432.14219667751

Table 6
The coefficients from the collocation Trefftz method by the central rule for Model I with u_L as $L=44$

i	$\hat{c}_1$	i	$\hat{c}_1$
1	0.43214219667770(2)	23	0.16489962791699(−5)
2	0.31260955885527(2)	24	−0.79051314384074(−6)
3	0.18038119234387(2)	25	0.37931215697053(−6)
4	−0.50111963888576(1)	26	0.18240663865146(−6)
5	0.25247674269181(1)	27	0.87840710016997(−7)
6	0.79217647609612	28	−0.42329123575021(−7)
7	0.31101912715291	29	0.20396909210300(−7)
8	−0.15593842689060	30	0.98583773313965(−8)
9	0.64666484264955(−1)	31	0.47728167326695(−8)
10	0.31023130031003(−1)	32	−0.23016373178046(−8)
11	0.14574593153069(−1)	33	0.10945497384787(−8)
12	−0.64753673008044(−2)	34	0.53140684243878(−9)
13	0.30355950425750(−2)	35	0.25906239084496(−9)
14	0.13875866526055(−2)	36	−0.12253369539977(−9)
15	0.64253903347776(−3)	37	0.52906242779061(−10)
16	−0.30356334877807(−3)	38	0.25805735672319(−10)
17	0.14229592607503(−3)	39	0.12740674743505(−10)
18	0.67458107151949(−4)	40	−0.56229016798380(−1 1)
19	0.32016503381154(−4)	41	0.16282561223942(−11)
20	−0.15178192325529(−4)	42	0.79889831908072(−12)
21	0.72347424374442(−5)	43	0.40231053525172(−12)
22	0.34495750578571(−5)	44	−0.15531526257412(−12)

Next for Model II, we should choose the partition in Fig. 8, and use the piecewise particular solutions (5.7). Both the central rule and the Gaussian rule of six nodes are employed to compute the integrals in (5.13). Denote by NNP the partition number of $A\bar{E}$ and $E\bar{D}$. In computation, we choose NNP as the multiple of six. The errors, condition numbers and the leading coefficients $\hat{c}_0$ are listed in Tables 7 and 8. For two integration rules, the errors and *Cond.* are slightly different, with the empirical rates:

$$\|\epsilon\|_{\mathrm{B}} = \mathrm{O}((0.55)^L), \quad Cond. = \mathrm{O}((1.27)^L). \tag{5.17}$$

Compared with (5.15), the condition numbers are significant smaller, while the errors retain the same high accuracy. The better performance in accuracy is also a development from the observation [5], based on the numerical data in [6].

Note that $\|\varepsilon\|_B$ in (5.17) displays the exponential convergence rates. It is proved in [9] that when the uniformly V_h elliptic inequality as well as the bilinear inequality is satisfied, the errors from the collocation Trefftz method are, basically (i.e. with a constant factor), the optimal truncation errors in (5.7), which have the exponential convergence rates for the harmonic functions on a sectorial domain, see Volkov [12], p. 41.

From Tables 7 and 8 the leading coefficient

$$\hat{d}_0 = 491.49398551255, \tag{5.18}$$

has 14 significant digits. When $L=24$, coefficient $\hat{d}_0$ has 9 and 12 significant digits from Tables 7 and 8, respectively. This implies that the Gaussian rule with six nodes provides better leading coefficients, the same conclusion made in [9].

Table 7
The error norms, condition numbers and the leading coefficient from the collocation Trefftz method for Model II by the central rule

L	N	M	NNP	$\|\varepsilon\|_B$	Cond.	$\hat{d}_0$
6	3	3	6	0.485	5.14	491.50375447935164
12	6	6	12	0.990(−2)	17.8	491.49403292439115
18	9	9	18	0.141(−3)	71.3	491.49398597288712
24	12	12	24	0.489(−5)	294	491.49398548887837
30	15	15	30	0.916(−7)	0.122(4)	491.49398551220833
36	18	18	36	0.371(−8)	0.514(4)	491.49398551257605
42	21	21	42	0.767(−10)	0.216(5)	491.49398551255416
48	24	24	48	0.354(−11)	0.916(5)	491.49398551255229

Table 8
The error norms, condition numbers and the leading coefficient from the collocation Trefftz method for Model II by the Gaussian rule of six nodes

L	N	M	NNP	$\|\varepsilon\|_B$	Cond.	$\hat{d}_0$	$\|\hat{d}_0 - \hat{d}_0\| \leq =48$
6	3	3	6	0.527	5.12	491.50984946552893	
12	6	6	12	0.959(−2)	17.0	491.49399162427318	0.00001172067
18	9	9	18	0.152(−3)	67.5	491.49398552412674	0.00000157423
24	12	12	24	0.454(−5)	278	491.49398551269798	0.00000014547
30	15	15	30	0.995(−7)	1.15(4)	491.49398551252898	0.00000002353
36	18	18	36	0.361(−8)	0.481(4)	491.49398551255371	0.00000000120
42	21	21	42	0.859(−10)	0.202(5)	491.49398551255291	0.00000000040
48	24	24	48	0.392(−11)	0.861(5)	491.49398551255251	0.00000000000

Hence, we list in Tables 9a and 9b the computed coefficients from the Gaussian rule with six nodes only. Besides, the leading coefficients $\hat{a}_1$ and $\hat{b}_0$ have 15 and 16 significant digits, given by:

$$\hat{a}_1 = -197.843688202747, \quad \hat{b}_0 = -108.3167742382339. \tag{5.19}$$

Moreover, we can see from $|\hat{d}_0 - \hat{d}_0| \leq =48$ in Table 8 that the leading coefficient $\hat{d}_0$ also has the exponential convergence rates,

$$\Delta d_0 = |\hat{d}_0 - d_0| = \mathrm{O}((0.56)^L).$$

Remark 6.1. In Tang [10], a number of singularity models for Laplace's equations on rectangle S with the

Table 9a
The coefficients d_i from the collocation Trefftz method by the Gaussian rule with six nodes for Model II with $L=42$, $M=21$ and $N=21$

i	$\hat{d}_i$	i	$\hat{d}_i$
0	0.49149398551255(3)	22	0.28296876209014(−3)
1	0.20065238223118(2)	23	0.17445041211420(−3)
2	−0.31336492129090(2)	24	−0.30575467669084(−3)
3	0.84502739982599(1)	25	0.19077594908752(−3)
4	0.15443903862693(2)	26	−0.50780058124318(−4)
5	−0.52203007093797(1)	27	−0.31978418070731(−4)
6	0.10853377508385(1)	28	0.55851059563915(−4)
7	0.45247368697120)	29	−0.35445135492159(−4)
8	−0.71447060802058)	30	0.95349846596053(−5)
9	0.34620015754709)	31	0.60578683131418(−5)
10	−0.75107200195077(−1)	32	−0.10476743650533(−4)
11	−0.39753375330083(−1)	33	0.66984928968357(−5)
12	0.82736452629329(−1)	34	−0.17784188813767(−5)
13	−0.45334765014809(−1)	35	−0.10897146397864(−5)
14	0.11220412185256(−1)	36	0.18351999362232(−5)
15	0.63615937532872(−2)	37	−0.11574049991123(−5)
16	−0.11139219730940(−1)	38	0.27828600655526(−6)
17	0.65343214462257(−2)	39	0.13463498937738(−6)
18	−0.16594741652122(−2)	40	−0.21339700669832(−6)
19	−0.99468983459638(−3)	41	0.12852559004887(−6)
20	0.17769148561836(−2)	42	−0.22265448089398(−7)
21	−0.10807339151966(−2)		

Table 9b
The coefficients a_i and b_i from the collocation Trefftz method by the Gaussian rule with six nodes for Model II with $L=42$, $M=21$ and $N=21$

i	$\hat{a}_i$	i	$\hat{b}_i$
1	−0.19784368820275(3)	0	−0.10831677423823(3)
2	−0.31926930057149(1)	1	0.29780407286597(2)
3	0.64293346822787(1)	2	0.12655253431819(2)
4	0.75030546466542	3	−0.144993897267l4(1)
5	−0.60862066562632	4	−0.10047797333552(1)
6	−0.92423658976556(−1)	5	0.15330929917106
7	0.93708777642456(−1)	6	0.14978794259931
8	0.15521001580253(−1)	7	−0.24773993470475(−1)
9	−0.15878893208957(−1)	8	−0.24629343903207(−1)
10	−0.27632100592619(−2)	9	0.42813849810836(−2)
11	0.29306574648338(−2)	10	0.44706691928972(−2)
12	0.52625553145008(−3)	11	−0.80216072455720(−3)
13	−0.56856704278497(−3)	12	−0.85704781612190(−3)
14	−0.10419605918837(−3)	13	0.15720069031688(−3)
15	0.11420949850474(−3)	14	0.17078652690669(−3)
16	0.20936766448185(−4)	15	−0.31858002906200(−4)
17	−0.23074560887560(−4)	16	−0.34434427308903(−4)
18	−0.38768970065648(−5)	17	0.65258826319999(−5)
19	0.42150857308363(−5)	18	0.63676400596069(−5)
20	0.47049774548533(−6)	19	−0.12273737750039(−5)
21	−0.49013499517408(−6)	20	0.76595590808321(−6)
		21	0.14902151022334(−6)

Table 10
The error norms, condition numbers and the leading coefficient from the collocation Trefftz method by the central rule for Model II by ignoring the mild singularities at the corners B and C

L	NNP	$\|\varepsilon\|_B$	Cond.	$\hat{d}_0^*$	$\|\hat{d}_0^* - d_0\|$
6	6	13.7	5.99	492.34847235119	
12	12	3.58	82.8	491.51252765213	0.185(−1)
18	18	1.71	636	491.50221240460	
24	24	0.863	0.720(4)	491.49869961824	0.471(−2)
30	30	0.583	0.513(5)	491.49694490581	
36	36	0.350	0.556(6)	491.49602070057	
42	42	0.262	0.385(7)	491.49546168905	
48	48	0.177	0.429(8)	491.49510320203	0.112(−2)

Dirichlet–Neumann boundary conditions are computed. The uniform admissible functions

$$v = \sum_{i=0}^{L} \mathrm{d}_i r^{i+(1/2)} \cos\left(i + \frac{1}{2}\right)\theta, \quad \text{in } S, \tag{5.20}$$

are chosen. When there is only one singularity at the origin, the very highly accurate solutions can be obtained by the collocation Trefftz method, and the exponential convergence rates are verified numerically. However, if there exists a mild singularity of $O(r^k \ln r)$, $k=1,2$ at corners, the accuracy of the numerical solutions is reduced significantly, and only the polynomial convergences rates can be observed. From Tang [10] we conclude that the divisions of S into three subdomains and the use of the piecewise admissible functions as (5.7) are absolutely necessary to achieve the highly accurate solutions by the collocation Trefftz method, and to retain the exponential convergence rates.

Now, we ignore the mild singularity at the corners B and C, choose the uniform functions (5.20) only in the entire domain, and carry out the collocation Trefftz method for Model II. The computed results are list in Table 10, and the leading coefficients in Table 11. From Table 10 we can see

$$\|\epsilon\|_B = O(L^{-2}), \quad Cond. = O((1.42)^L), \tag{5.21}$$

by noting the ratio from the data in Table 10:

$$\frac{(\|\varepsilon\|_B)_{L=24}}{(\|\varepsilon\|_B)_{L=48}} = \frac{0.863}{0.177} = 4.88 = 2^{2.28}.$$

The convergence rate $O(L^{-2})$ is polynomial and slow; while the condition numbers significantly larger than those in (5.17). In Babuska and Guo [2], for the mild singularity $O(r^k \ln r)$, the polynomial convergence rates

$$\|\varepsilon\|_{1,S} = O(L^{-2k}), \tag{5.22}$$

are proved for the p-version FEM. Since there is a mild singularity $O(\xi \ln \eta)$ at corner C in Model II, the convergence rate $O(L^{-2})$ coincides with (5.22) very well. Interestingly, although the slow convergence rates occur, the leading coefficients, $\hat{d}_0^*$ and $\hat{d}_1^*$, still have five and four significant digits. This implies that the solutions near the origin may not be influenced strongly by the mild singularity at the far away corners. However, the convergence rates for $\hat{d}_0^*$ is also polynomial

$$\Delta\hat{d}_0^* = O(L^{-2}), \tag{5.23}$$

by comparing $\hat{d}_0^*$ in Table 10 with $\hat{d}_0$ in (5.18)

$$\frac{|\hat{d}_0 - \hat{d}_0^*|_{L=24}}{|\hat{d}_0 - \hat{d}_0^*|_{L=48}} = \frac{0.471(-2)}{0.112(-2)} = 4.21 = 2^{2.07}.$$

6. Concluding remarks

To close this paper, let us give a few remarks.

1. The particular solutions of Poisson's and Laplace's equations on a sector with the Dirichlet, the Neumann boundary conditions, and their mixed types are derived in detail. Although these solutions can be found in Volkov

Table 11
The coefficients $\hat{d}_i^*$ from the collocation Trefftz method by the central rule for Model II with $L=42$ by ignoring the mild singularities at corners B and C

i	$\hat{d}_i^*$	i	$\hat{d}_i^*$
0	0.49149546168905(3)	22	−0.38732308021276(−2)
1	0.20061741631796(2)	23	0.15222922823156(−1)
2	−0.31332682690943(2)	24	−0.18537659186308(−1)
3	0.84476705355138(1)	25	0.13164570233705(−1)
4	0.15444654497322(2)	26	−0.36127640611058(−2)
5	−0.52197549909606(1)	27	0.13507935540894(−1)
6	0.10843997742414(1)	28	−0.15269033237590(−1)
7	0.45314965063084	29	0.97379816592412(−2)
8	−0.71469113400049	30	−0.14839402178926(−2)
9	0.34610701298805	31	0.64905517111838(−2)
10	−0.74935909769621(−1)	32	−0.70035779273999(−2)
11	−0.39632984998754(−1)	33	0.41042351379424(−2)
12	0.82256535112322(−1)	34	−0.25528371216394(−3)
13	−0.44645267648607(−1)	35	0.15575280684639(−2)
14	0.10533093384599(−1)	36	−0.16258709839073(−2)
15	0.88658956518358(−2)	37	0.89428271787672(−3)
16	−0.14897241354148(−1)	38	0.24127768058350(−5)
17	0.10194437974102(−1)	39	0.14814295972461(−3)
18	−0.40342227174215(−2)	40	−0.15230483989584(−3)
19	0.77421337052198(−2)	41	0.80339732143722(−4)
20	−0.98722765968634(−2)	42	0.31972123443789(−5)
21	0.84599449662161(−2)		

[11,12]. The solution formulas of harmonic functions given in this paper are more explicit, and easier to expose the mild singularity at the domain corners than those in [12]. A number of useful particular solutions for the rectangular, the L-shaped and the cracked domains are derived. Obviously, the analysis in this paper is also more comprehensive and complete than that in [5,7]. Choosing a set of good basis functions, in particular those representing singularities, is essential for the collocation Trefftz method. Hence, the analysis of the particular solutions in this paper will promote the collocation Trefftz method to a high capacity to solve the Poisson and Laplace equations on a polygon.

2. The particular solutions can exhibit a clear view of regularity and singularity. In this paper, we provide the particular solutions on special angles, $\Theta = i\pi/2$, $\Theta = (2i-1)\pi/4$, $i = 1$–4. Those solution behavior is important for the choices of numerical methods, because different numerical methods need different regularities of the true solution. Take linear finite element method and the finite difference method as examples. If $u \in H^2(S)$, the optimal convergence rate can be obtained, where $H^k(S)$ is the Sobolev space (cf. Ciarlet [4]). If $u \in H^3(S)$, the superconvergence of FDM may be achieved, see Li et al. [8]. Moreover, the existence of singularity may suggest that whether the refinement of elements is employed or not, and where this refinement should take place. When multi-singularities occur, the division of S should also be considered, and combinations of numerical treatments must be used. In summary, the particular solutions in this paper are imperative for numerical methods, not only for the collocation Trefftz method, but also to other methods, such as the combined method in [5] and the Schwarz alternating method.
3. Two new singularity models are designed, to include the discontinuity, and the crack plus the mild singularities of $O(r^k \ln r)$, $k = 1,2$. The high accurate solutions of exponential convergence rates are also provided by the collocation Trefftz method, which can be regarded as the 'true' solution for testing other numerical methods. By using piecewise particular solutions in subdomains, not only can the condition numbers be reduced significantly, but also the high accuracy of the solutions may be achieved as well. This is a new discovery, compared with [5]. Moreover, the Gaussian rule with high order may raise the accuracy of the leading coefficients; this is also coincident with [9].
4. Highly accurate collocation Trefftz method in [9] can be extended to the complicated problems by using the piecewise particular solutions as shown in Model II, or by employing the Schwarz alternating method. For Model II, let S be divided into three overlapped subdomains S_0, S_1, and S_2 in Fig. 10. We may carry out the collocation Trefftz method in each S_i including just one singularity, and use a few iterations to provide the solutions of Model II having the exponential convergence rates. Numerical results will report elsewhere.

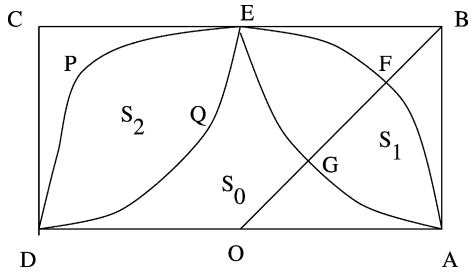

Fig. 10. Overlapped subdomains of S.

References

[1] Babuska I, Aziz AK. Part I, Survey lectures on the mathematical foundations of the finite element method. In: Aziz AK, editor. The mathematical foundations of the finite element with applications to partial differential equations. New York: Academic Press, Inc.; 1971. p. 3–358.
[2] Babuska I, Guo B. Part I, Approximability of functions on the weighted Besov space, Direct and inverse approximation theorems for the p-version of the finite element method in the framework of weighted Besov space. Technical report. Canada: Department of Mathematics, University of Manitoba; 2001.
[3] Cheng AH-D, Lafe O, Grilli S. Dual-reciprocity BEM based on global interpolation functions. Eng Anal Bound Elem 1994;13:303–11.
[4] Ciarlet PG. Basic error estimates for elliptic problems. In: Ciarlet PG, Lions JL, editors. Finite element methods (Part I). Amsterdam: North-Holland; 1991. p. 17–351.
[5] Li ZC. Combined methods for elliptic equations with singularities, interfaces and infinities. Dordecht, MA: Kluwer Academic Publisher; 1998.
[6] Li ZC, Mathon R, Sermer P. Boundary methods for solving elliptic problem with singularities and interfaces. SIAM J Numer Anal 1987; 24:487–98.
[7] Li ZC, Lu TT. Singularities and treatments of elliptic boundary value problems. Math Comput Modell 2000;31:97–145.
[8] Li ZC, Yamamoto T, Fang Q. Superconvergence of solution derivatives for the Shortly-Weller difference approximation of Poisson's equation, Part I, Smoothness problems. J Comput Appl Math 2003;151:307–33.
[9] Lu TT, Hu HY, Li ZC. Highly accurate solutions of Motz's and the cracked beam problems. Eng Anal Bound Elem 2004 in press.
[10] Tang LD. Cracked beam and related singularity problems. Master Thesis, Department of Applied Mathematics, National Sun Yat-sen University; June 2001.
[11] Volkov EA. An exponentially convergent method for the solution of Laplace's equation on polygons. Math USSR Sbornik 1980;37(3).
[12] Volkov EA. Block method for solving the Laplace equation and for constructing conformal mappings. Boca Raton: CRC Press; 1994.